

# LGTM: Local-to-Global Text-Driven Human Motion Diffusion Model

Haowen Sun  
Shenzhen University  
China  
zover.v@gmail.com

Ruikun Zheng  
Shenzhen University  
China  
zhengzrk@gmail.com

Haibin Huang  
Kuaishou Technology  
China  
jackiehuanghaibin@gmail.com

Chongyang Ma  
ByteDance Inc.  
USA  
chongyangm@gmail.com

Hui Huang  
Shenzhen University  
China  
hhzhiyan@gmail.com

Ruizhen Hu\*  
Shenzhen University  
China  
ruizhen.hu@gmail.com

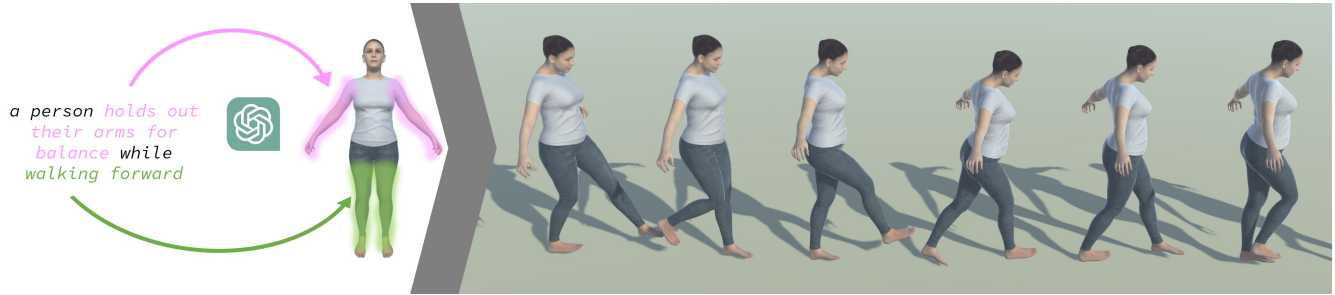


**Figure 1: LGTM decomposes input text description at the part level using LLMs and generates output motion from local to global with both part description and full-body descriptions.**

## ABSTRACT

In this paper, we introduce LGTM, a novel Local-to-Global pipeline for Text-to-Motion generation. LGTM utilizes a diffusion-based architecture and aims to address the challenge of accurately translating textual descriptions into semantically coherent human motion in computer animation. Specifically, traditional methods often struggle with semantic discrepancies, particularly in aligning specific motions to the correct body parts. To address this issue, we propose a two-stage pipeline to overcome this challenge: it first employs large language models (LLMs) to decompose global motion descriptions into part-specific narratives, which are then processed by independent body-part motion encoders to ensure precise local semantic alignment. Finally, an attention-based full-body optimizer refines the motion generation results and guarantees the overall coherence. Our experiments demonstrate that LGTM gains significant improvements in generating locally accurate, semantically-aligned human motion, marking a notable advancement in text-to-motion applications. Code and data for this paper are available at <https://github.com/L-Sun/LGTM>

## CCS CONCEPTS

• **Computing methodologies** → **Motion processing.**

## KEYWORDS

Motion Synthesis; Diffusion Model; Text-Driven Generation.

## 1 INTRODUCTION

In this paper, we address the problem of text-to-motion, *i.e.*, given a textual description of movements for a character, we aim to automatically generate plausible and realistic 3D human motions. The successful automation of this process holds significant potential for a variety of downstream applications, including the creation of content for augmented and virtual reality environments, advancements in robotics, and enhancements in human-machine interactions [Chen et al. 2021; Lan et al. 2023; Scanlon et al. 2023; Zhao et al. 2022].

As a longstanding challenge at the confluence of natural language processing, machine learning, and computer graphics, text-to-motion generation has garnered significant attention in recent research [Jiang et al. 2023; Petrovich et al. 2022; Tevet et al. 2022a]. The advent of diffusion models, as highlighted in various studies [Alexanderson et al. 2023; Poole et al. 2022; Rombach et al. 2022], has propelled notable advancements in this field [Tevet et al. 2022b]. Despite these strides, the task of generating motions that are both locally semantic accurate and globally coherent from textual descriptions remains a formidable hurdle. Current methods often face difficulties in effectively capturing the nuanced local semantics embedded in motion descriptions and in producing motions that align accurately with these semantic cues.

In particular, existing approaches in text-to-motion synthesis often encounter issues such as local semantic leakage and missing elements [Chen et al. 2023a; Tevet et al. 2022b]. For instance, when prompted with a description like “a man kicks something with his left leg”, these methods might erroneously generate a motion that

\*Corresponding author: Ruizhen Hu (ruizhen.hu@gmail.com)

corresponds to a “right kick”. Similarly, prompts involving complex actions requiring coordination of multiple body parts frequently result in motions with certain parts omitted. Our observations reveal two primary shortcomings in these methods. Firstly, most existing techniques utilize a single global text descriptor for all local body motions. This approach requires the network to learn the association between local motion semantics and respective body parts from a unified global text source. This process proves challenging, especially when the textual content bears similarity across different body parts, leading to difficulties in differentiating specific actions for each part. Secondly, the text encoders used in these methods exhibit limited effectiveness in encoding motion-related text. This limitation is apparent in the high feature similarity observed among different motion texts, as detailed in recent studies [Petrovich et al. 2023]. This homogeneity in encoded text features further exacerbates the network’s struggle to discern and accurately represent subtle variations in local textual semantics.

Towards this end, we present a novel diffusion-based text-to-motion generation architecture, LGTM, adept at producing motions that are both in alignment with textual descriptions and precise in local semantic accuracy. LGTM operates through a local-to-global approach, structured in two main stages. The first stage implements an efficient strategy to tackle the issue of local semantic accuracy. Here, we introduce a partition module that employs large language models (LLMs) to dissect global motion descriptions into narratives specific to each body part. Subsequently, dedicated body-part motion encoders independently process these part-specific narratives. This focused approach effectively circumvents local semantic inaccuracies by reducing redundant information and preventing semantic leakage, thus maintaining a sharp focus on relevant local semantics. However, as each body-part motion encoder functions independently, without awareness of other parts’ movements, it is imperative to synchronize these individual motions to avoid full-body coordination issues. To address this, the second stage of LGTM introduces an attention-based full-body optimizer. This component is specifically designed to facilitate the integration of information among different body parts, ensuring that the overall motion is not only locally precise but also globally coherent and fluid.

To evaluate the effectiveness of LGTM, we further conduct experiments on text-driven motion generation and provide both quantitative and qualitative results. Our experiments show that our proposed LGTM can generate faithful motions that better align with the input text both locally and globally, and outperform state-of-the-art methods.

To summarize, our contributions are as follows:

- We present LGTM, a novel diffusion-based architecture that translate textual descriptions into accurate and coherent human motions, marking a significant improvement over previous text-to-motion approaches.
- LGTM introduces a unique partition module that utilizes LLMs to decompose complex motion descriptions into part-specific narratives. This significantly enhances local semantic accuracy in motion generation.
- Our experiments demonstrate the effective integration of independent body-part motion encoders with an attention-based full-body optimizer, ensuring both local precision and global

coherence in generated motions, providing a promising improvement for text-to-motion generation.

## 2 RELATED WORK

The generation of motion sequences is a longstanding challenge within the domain of computer graphics, where the objective is to produce a series of motion frames guided by conditional control signals. Given that our approach is centered on body-partition-based text-to-motion synthesis, we explore relevant literature across two primary aspects: body partition modeling and text-to-motion generation.

*Part-based motion modeling.* Partitioning the human body into distinct segments facilitates the control of motion synthesis at a more granular level, allowing for localized adjustments.

Several studies have explored the concept of combining motions of individual body parts to synthesize novel motions. [Hecker et al. 2008] introduced a retargeting algorithm that composes motions at the level of individual body parts to generate diverse character animations. [Jang et al. 2008] divided motions into upper and lower body segments, merging them through an algorithm to augment their motion database. [Soga et al. 2016] synthesized dance motions from existing datasets by focusing on body partitions. [Jang et al. 2022] performed style transfer at the part level, utilizing a graph convolutional network to assemble different body part motions into new, coherent sequences, preserving local styles while transferring them to specific body parts without compromising the integrity of other parts or the entire body. However, these methods rely on pre-existing motion data, and hence are more accurately described as synthesis rather than generation.

For more detailed local control, [Starke et al. 2020] proposed a local phase model based on body partitions used to generate basketball player movements, achieving higher local fidelity compared to global phase approaches [Starke et al. 2019; Zhang et al. 2018]. [Starke et al. 2021] introduced a neural animation layering technique that combines trajectories of different body parts produced by control modules, providing animators with more granular control and enabling the creation of high-quality motion. [Lee et al. 2022] developed an algorithm for reassembling physically-based part motions, allowing the combination of partial movements from characters with varying skeletal structures. By operating in a physically simulated virtual environment, they employed part-wise timewarping and optimization-based assembly to ensure improved spatial and temporal alignment. [Bae et al. 2023] utilized part-wise motion discriminators to enhance motion variety and a global control policy to maintain the physical realism of the movements.

*Text-to-motion generation.* Text provides a user-friendly interface for directing motion generation due to its ease of use and editing capabilities. However, a significant challenge arises from the difficulty in precisely controlling the outcome of the generated motion through text. In this subsection, we examine text-to-motion generation techniques and identify their limitations.

Certain text-to-motion approaches are founded on the encoder-decoder architecture and focus on aligning modalities within a unified latent space. [Ahuja and Morency 2019] trained their network by alternating between encoding motions and texts, then

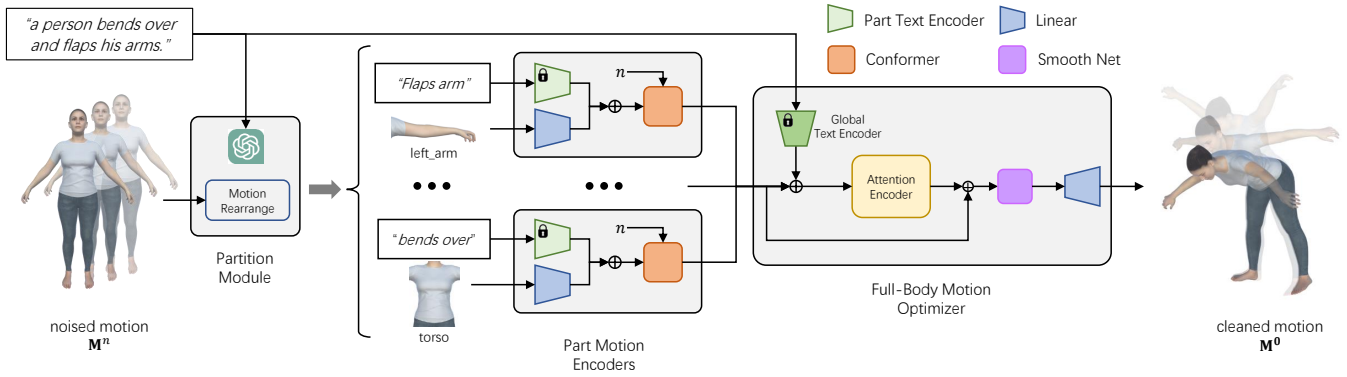


**Figure 2: Overview of our LGTM framework, which consists of three major components. (1) The partition module utilizes ChatGPT to deconstruct motion descriptions  $T$  into body part level text  $T_{\text{part}}$ , and decomposes full-body motion  $M$  to body part motion  $M_{\text{part}}$ ; (2) The part motion encoders encodes part-level motions with corresponding part-level text independently and a diffusion time step  $n$ ; (3) The full-body motion optimizer utilizes an attention module to optimize fused body part motion with full-body text semantic.**

decoding them back into motion, thereby implicitly aligning the two modalities. [Ghosh et al. 2021; Petrovich et al. 2022] encoded text and motion concurrently and decoded them into motion, employing additional loss functions to bring the modalities closer within the latent space. These methods struggle with generating motions from lengthy textual descriptions. [Athanasios et al. 2022] tackled long motion generation by producing short motion clips in an auto-regressive fashion, but this requires manual segmentation of long textual descriptions into shorter segments and specification of action duration. To utilize visual priors, [Tevet et al. 2022a] employed a frozen CLIP [Radford et al. 2021] text encoder to encode motion descriptions and aligned the motion latent space with that of CLIP. Nevertheless, the images used for alignment, rendered from random motion frames, can confuse the network when the frames are not representative. Moreover, [Petrovich et al. 2023] observed that motion descriptions tend to cluster closely in the CLIP latent space, as the distribution of motion-related text is narrower than that of the broader text datasets used to train CLIP.

Recent developments in neural diffusion models for image generation have inspired text-to-motion methods that leverage these models to achieve superior quality. [Tevet et al. 2022b; Zhang et al. 2022] utilized Transformer to denoise motion conditioned on text. [Chen et al. 2023b] introduced a U-Net-based DDIM generative model to denoise motion in latent space, resulting in expedited generation. However, these methods lack the ability to control localized motion generation through masking. Additionally, they struggle to learning correct mapping of the local semantics because all body parts share the same textual information, which potentially lead to semantically mismatched part motions.

An alternative approach to motion generation involves processing motion in a discrete space through token prediction [Guo et al. 2022b; Jiang et al. 2023; Yao et al. [n. d.]]. But the limitations of these works are that the expressive capacity of the codebook can restrict the diversity of the generated motions, potentially causing the text input to be mapped to unintended motions.

The challenges in controlling local motion semantics stem from: (1) the sharing of textual information across all body parts, and (2) the difficulty networks face in distinguishing text latent codes encoded by CLIP. These factors contribute to the difficulty of achieving precise local semantic control in motion generation, leading to issues such as semantic leakage.

Drawing inspiration from the technological advancements and challenges identified in prior research, we propose a novel framework that combines body-part partitioning with independent local motion semantic injection and a global semantic joint optimization strategy. This framework is designed to enhance the fidelity and controllability of text-to-motion synthesis, addressing the need for more nuanced and accurate motion generation.

### 3 METHOD

In this section, we delve into the specifics of LGTM, as illustrated in Figure 2. LGTM is structured as a local-to-global generation framework that initially creates local, part-level motion, followed by a global fusion and optimization process to produce the final full-body motion. At its core, LGTM operates by subdividing the full-body text and motion spaces into body-part-specific subspaces. Such subdivision is adeptly handled by a dedicated Partition Module.

For each of these subspaces, we have developed specialized part motion encoders. These encoders are trained to learn independently a series of mappings between part-level motions and part-level text. This strategy effectively mitigates the issues of incorrect local semantic mapping seen in previous methods. Following the localized encoding, LGTM introduces a full-body motion optimizer to establish correlations among the various subspaces and ensure the consistency and coherence of the final full-body motion. Below, we provide a detailed explanation of the functionalities and details of each module in LGTM.

### 3.1 Preliminary: Human Motion Diffusion Model

*Input representation.* We define the input pair for our method as  $(\mathbf{M}, T)$ , where  $\mathbf{M}$  represents full-body motion data and  $T$  denotes the raw full-body text description. Specifically, we use the HumanML3D representation proposed by [Guo et al. 2022a] as our motion data representation, which is calculated from the SMPL motion data [Loper et al. 2015] and includes redundant motion features that are helpful for network training. A full-body motion data  $\mathbf{M}$  contains  $F$  frames and  $J = 22$  joints. Specifically, we denote  $\mathbf{M} = [\dot{\mathbf{r}}_{\text{root}}, v_{\text{root}}, \mathbf{h}, \mathbf{p}, \mathbf{r}, \mathbf{v}, \mathbf{c}]$ , where  $\dot{\mathbf{r}}_{\text{root}} \in \mathbb{R}^{F \times 1}$ ,  $v_{\text{root}} \in \mathbb{R}^{F \times 2}$  and  $\mathbf{h} \in \mathbb{R}^{F \times 1}$  are the angular velocity around y-axis, linear velocity on x-z plane, and height of the root joint,  $\mathbf{p} \in \mathbb{R}^{F \times (J-1) \times 3}$  and  $\mathbf{r} \in \mathbb{R}^{F \times (J-1) \times 6}$  are local position and 6D rotation [Zhang et al. 2018] of all joints except root joint,  $\mathbf{v} \in \mathbb{R}^{F \times J \times 3}$  is the local velocity of all joints, and  $\mathbf{c} \in \mathbb{R}^{F \times 4}$  is the contact signal of feet.

*Diffusion model.* Our method is built upon a text-conditional diffusion model. In the training stage, this model adds noise to a clean motion  $\mathbf{M}$  following the Markov process and trains a network to predict the added noise with an L2 loss. In the sampling stage, this model gradually reduces noise from a purely noised motion  $\mathbf{M}^n$  with the predicted noise. We use the DDIM [Song et al. 2022] as our diffusion model to accelerate the sampling process. More details is provided in the supplementary material.

### 3.2 Partition Module

The Partition Module is designed to inject local semantics into each body part for Part Motion Encoders. In practice, an input pair  $(\mathbf{M}, T)$  is divided into six parts, including *head*, *left arm*, *right arm*, *torso*, *left leg*, and *right leg*.

The motion  $\mathbf{M}$  is decomposed as follows:

$$\begin{aligned} \mathbf{M}_{\text{head}} &= [\mathbf{p}_{\text{head}}, \mathbf{r}_{\text{head}}, \mathbf{v}_{\text{head}}] \in \mathbb{R}^{F \times 24} \\ \mathbf{M}_{\text{left\_arm}} &= [\mathbf{p}_{\text{left\_arm}}, \mathbf{r}_{\text{left\_arm}}, \mathbf{v}_{\text{left\_arm}}] \in \mathbb{R}^{F \times 48} \\ \mathbf{M}_{\text{right\_arm}} &= [\mathbf{p}_{\text{right\_arm}}, \mathbf{r}_{\text{right\_arm}}, \mathbf{v}_{\text{right\_arm}}] \in \mathbb{R}^{F \times 48} \\ \mathbf{M}_{\text{torso}} &= [\mathbf{p}_{\text{torso}}, \mathbf{r}_{\text{torso}}, \mathbf{v}_{\text{torso}}, \dot{\mathbf{r}}_{\text{root}}, v_{\text{root}}, \mathbf{h}] \in \mathbb{R}^{F \times 43} \\ \mathbf{M}_{\text{left\_leg}} &= [\mathbf{p}_{\text{left\_leg}}, \mathbf{r}_{\text{left\_leg}}, \mathbf{v}_{\text{left\_leg}}, \mathbf{c}_{\text{left\_leg}}] \in \mathbb{R}^{F \times 50} \\ \mathbf{M}_{\text{right\_leg}} &= [\mathbf{p}_{\text{right\_leg}}, \mathbf{r}_{\text{right\_leg}}, \mathbf{v}_{\text{right\_leg}}, \mathbf{c}_{\text{right\_leg}}] \in \mathbb{R}^{F \times 50}, \end{aligned}$$

where the subscript indicates where the feature from. For example,  $\mathbf{p}_{\text{right\_leg}}$  includes all local positions of joints from the *right leg*.

For the motion description  $T$ , we leverage the knowledge inference capabilities of LLMs to decompose it into six parts:  $T_{\text{head}}$ ,  $T_{\text{left\_arm}}$ ,  $T_{\text{right\_arm}}$ ,  $T_{\text{torso}}$ ,  $T_{\text{left\_leg}}$  and  $T_{\text{right\_leg}}$  using crafted prompts. The prompt includes three sections: task definition, output requirements, and some output examples. The task definition instructs LLMs to extract principal descriptions for each motion part. The output requirements tell LLMs that we need structured output such as JSON format, body part naming, etc. Then, we employ a few-shot approach to guide LLMs in generating the desired output. More details of our prompts can be found in the supplementary materials. A decomposed description example is shown in Table 1.

**Table 1: An example of decomposing full-body motion description: “a person waves the right hand and then slightly bends down to the right and takes a few steps forward.”**

Part name	Part description
head	dose nothing
left arm	dose nothing
right arm	waves hand
torso	slightly bends down
left leg	takes a few steps forward
right leg	takes a few steps forward

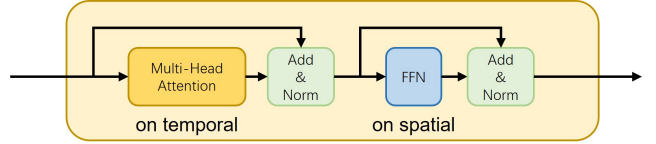


**Figure 3: The structure of an attention encoder block.**

### 3.3 Part Motion Encoders

The part motion encoders,  $\{E_{\text{head}}, \dots, E_{\text{right\_leg}}\}$ , aim to learn local semantic mapping from part-level input pairs  $(\mathbf{M}_{\text{part}}^n, T_{\text{part}})$  independently. Since each encoder obtains information only from its corresponding part-level input pair and cannot access information from other body parts, the issue of semantic leakage is effectively alleviated. We denote the part-level encoding process as follows:

$$\mathbf{z}_{\text{part}}^n = E_{\text{part}}(\mathbf{M}_{\text{part}}^n, T_{\text{part}}, n), \quad (1)$$

where each part motion encoder,  $E_{\text{part}}$ , consists of three components: a linear layer, a text encoder, and a Conformer [Gulati et al. 2020]. The linear layer aims to align the size of the latent dimension with that of the text encoder. We use six different frozen part-level TMR text encoders [Petrovich et al. 2023], each corresponding to one of the six body parts, which are pretrained on part-level motion-text pairs  $(\mathbf{M}_{\text{part}}, T_{\text{part}})$  respectively. Since the TMR model is trained only on motion description and motion data, and not on large visual datasets, the motion-related text embedding encoded by TMR is easier for the network to distinguish than that by CLIP. The projected motion and text embedding are then fused and processed by a Conformer [Gulati et al. 2020]. The Conformer incorporates convolution blocks into the Transformer [Vaswani et al. 2017] architecture to better capture temporal local features. Moreover, previous work [Alexanderson et al. 2023] shows the success of Conformer on music-to-dance task.

### 3.4 Full-Body Motion Optimizer

Since each part’s motion and text are independently encoded to  $\{\mathbf{z}_{\text{head}}^n, \dots, \mathbf{z}_{\text{left\_leg}}^n\}$  independently, the network will ignore the correlations between the different body parts, therefore, we propose that the full-body motion optimizer  $G$  establishes correlations by adjusting the movements of each body part based on full-body text information.

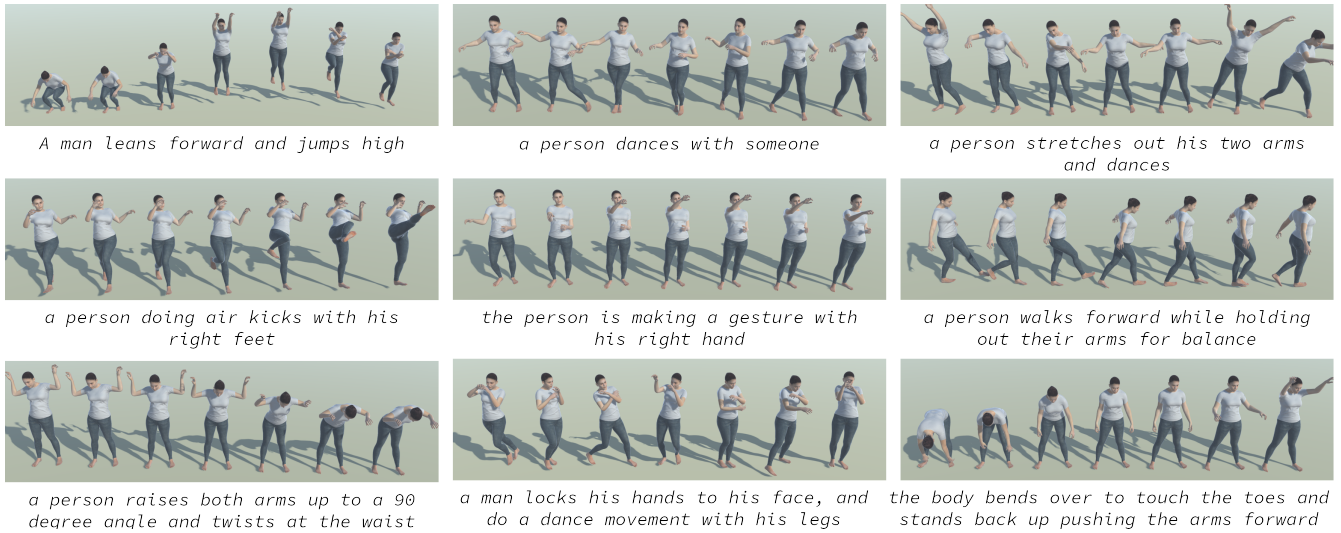


Figure 4: Example results generated by our method.

Specifically, we first concatenate all body part latent codes into a full-body latent code  $\mathbf{z}^n$  whose shape is  $(F, S) = (F, 6 \times 128)$ , and then fuse it with the global text embedding encoded by freezing the full-body level TMR text encoder. Next, we use an attention encoder [Vaswani et al. 2017] to compute a delta that adjusts each part in the latent code  $\mathbf{z}^n$ . The attention encoder is where the exchange of spatio-temporal information actually occurs. It consists of several attention encoder blocks, each containing a multi-head attention block and a feed-forward layer, as shown in Figure 3. Since the latent code  $\mathbf{z}^n$  is processed by a multi-head attention block on the temporal dimension  $F$ , and feed-forward layers (FFN) operate on the spatial dimension  $S$ , the latent code for each body part can continuously exchange temporal and spatial information. Next, we use a SmoothNet [Zeng et al. 2022] to reduce jitter, which contains a stacked MLP with residual connections and operates on the temporal dimension, acting as a low-pass filter in the latent space.

Finally, we project the latent code to origin feature dimension, and get a clean motion  $\hat{\mathbf{M}}^0$ . The full-body motion optimizer can be formulated as

$$\hat{\mathbf{M}}^0 = G(\mathbf{z}_{\text{head}}^n, \dots, \mathbf{z}_{\text{left\_leg}}^n, T) = \text{Linear}(\text{SmoothNet}(\mathbf{z}^n + \text{AttentionEncoder}(\mathbf{z}_{\text{text}} + \mathbf{z}^n))) \quad (2)$$

## 4 RESULTS

In this section, we present the motions generated by our method and conduct a comparative analysis with other text-driven motion generation methods. Additionally, we perform several ablation studies to highlight the contributions of individual components within our framework.

### 4.1 Implementation Details

The part-level motion description is generated by ChatGPT. (*gpt-3.5-turbo-1106*) model. Our model is trained with AdamW optimizer with learning rate decaying strategy of fast warm cosine decay. The

initial learning rate is  $10^{-4}$  and the batch size is 64. The number of diffusion steps is 1K. The training time of our model on the HumanML3D dataset is about 8 hours on 3 NVIDIA RTX 4090 GPUs.

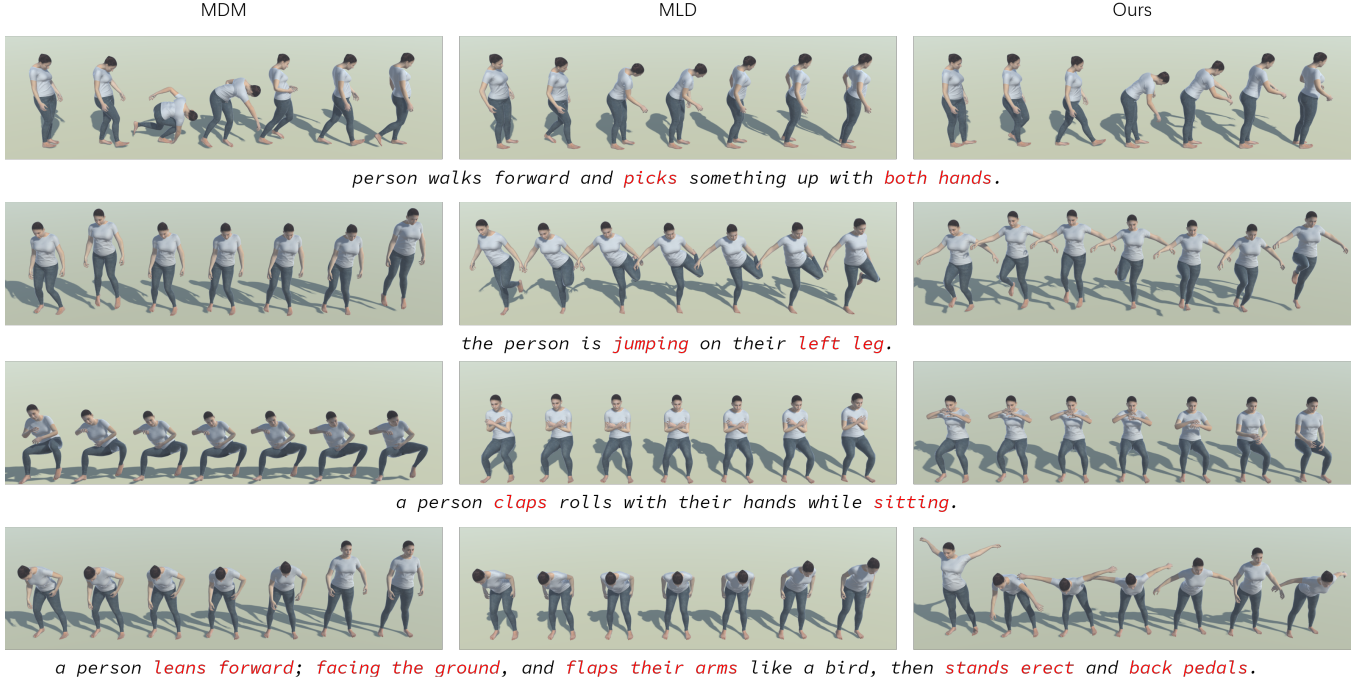
### 4.2 Qualitative Results

Figure 4 shows several example results generated by our method. We can see that our method can generate motion with precise local semantics, such as body part semantic correspondence and action timing order, as our method injects local semantic information into corresponding parts independently, and the whole-body optimizer builds correct relationships between body parts in both spatial and temporal domains. For example, the result of “*a man leans forward and jumps high*” shows that the character does *lean* and *jump* in the correct order. The result of “*a man lock his hands to his face, and do a dance move net with his legs*” shows that the character keeps correct spatial relationship between hand and face while dancing. The result of “*a person doing air kicks with his right feet*” shows that the character do *kick* with correct body part.

We also provide some visual comparisons to two baselines, including MDM [Tevet et al. 2022b] and MLD [Chen et al. 2023b]. Figure 5 shows that our method can generate more semantic well-matched motion. In the first row, the character can pick something with *both hands* in our result, but with just left hand in MDM. In the second row, the character only jumps on the left foot correctly in our result, but jumps on both feet in MDM and dose not jump in MLD. In the third row, the result of MDM contains weird pose and the MLD dose not contain “claps”, but our result is more correct. The last row shows that, for more complex text inputs, our method is able to generate more semantic accurate results than those two baselines.

### 4.3 Quantitative Evaluation

*Evaluation metrics.* To quantitatively evaluate our method, we use the metrics suggested by [Guo et al. 2022a] which includes



**Figure 5: Qualitative comparison of results generated by our method with those from MDM [Tevet et al. 2022b] and MLD [Chen et al. 2023b].**

(1) **Fréchet Inception Distance (FID)** that evaluates the generated motion quality against real motion distribution; (2) **Diversity (DIV)** that calculates the variance of generated motion; (3) **R Precision** that calculates the top-n matching accuracy between generated motion and the corresponding text description; (4) **Multi-Modal Distance (MM Dist)** that calculates the distance between paired motion and text; (5) **Part-level Multi-Modal Similarity (PMM Sim)** that calculates the normalized cosine similarity between part-level paired motion and text. These metrics are calculated in the latent space using the text encoder and motion encoder from T2M [Guo et al. 2022a] as in previous works. As our method provides detailed control of generated motions, we also compare our method to baselines in terms of part-level motion quality using Part-level Multi-Modal Similarity (PMM Sim), by training both part-level text encoder and motion encoder with contrastive learning as in TMR [Petrovich et al. 2023], which we believe makes motion samples in the latent space more dispersed allowing dissimilar motions can be distinguished more easily. Specifically, we calculate the PMM Sim in the TMR latent space as follows:

$$s_{\text{part}} = \frac{1}{2} \left( \frac{z_{\text{part}}^{\text{M}} \cdot z_{\text{part}}^{\text{T}}}{\|z_{\text{part}}^{\text{M}}\| \|z_{\text{part}}^{\text{T}}\|} + 1 \right) \quad (3)$$

where both  $z_{\text{part}}^{\text{M}}$  and  $z_{\text{part}}^{\text{T}}$  are obtained by encoding part-level motion and text through TMR encoders. Although we mainly focus on semantically controllable generation, we also evaluate common artifacts in text-to-motion synthesis. We assess the generated motions using three specific metrics: sliding, penetration, and floating, as introduced by [Yuan et al. 2022].

*Comparison results.* The comparison results for full-body motion are presented in Tables 2, and the comparison results for part-level motion are presented in Table 3. The FID and DIV in Tables 2 indicate that our method generates more realistic and diverse motion. The R Precision and MM Dist indicate that our method can generate better globally semantically matching motion. Table 3 also shows that our method achieves the best local semantic matching, with performance very close to that of real data. Our local-to-global design injects local semantic information independently into body parts and refines it with global semantics, which provides more accurate and structured semantic information to the network to help generation and thus achieve higher quality. For artifact evaluation, as shown in Table 4, we can see that each method exhibits performance very close to the ground truth (the Real row) at the millimeter scale. The artifacts can be attributed to the dataset’s intrinsic quality variances.

#### 4.4 Ablation Studies

We have designed two main experiments to assess the impact of different components of our approach. The first experiment investigates the influence of different text encoders on the motion quality. The second experiment evaluates the effect of the full-body motion optimizer on the the quality of motions generated by our method.

*The importance of text encoder.* We test our method by replacing our pre-trained text encoder with CLIP as an alternative, demonstrating that the TMR text encoder we use can capture more detailed semantics. Furthermore, we also present the results obtained by MDM using either CLIP or the TMR text encoder for comparison.

**Table 2: Comparison of the visual quality and degree of semantic matching between input text and output full-body motion. These metrics are computed in the latent space of the T2M model [Guo et al. 2022a].**

Method	FID ↓	DIV ↑	R Precision ↑			MM Dist ↓
			Top 1	Top 2	Top 3	
Real	0.000	9.831	0.513	0.708	0.804	2.939
MotionDiffuse[2022]	0.687	8.894	0.318	0.531	0.677	3.118
MDM[2022b]	0.747	9.462	0.390	0.581	0.695	3.635
MLD[2023b]	1.753	8.970	0.383	0.573	0.687	3.682
Ours (LGTM)	<b>0.218</b>	<b>9.638</b>	<b>0.490</b>	<b>0.689</b>	<b>0.788</b>	<b>3.013</b>

**Table 3: Comparison of text-to-motion generation using PMM Sim. These metrics are calculated in the latent space of the part-level TRM encoder. Higher values indicate better performance.**

Method	head	left arm	right arm	torso	left leg	right leg
Real	0.803	0.716	0.723	0.759	0.755	0.760
MotionDiffuse[2022]	0.789	0.687	0.712	0.735	0.728	0.739
MDM[2022b]	0.783	0.699	0.691	0.740	0.717	0.723
MLD[2023b]	0.771	0.675	0.702	0.717	0.723	0.726
Ours (LGTM)	<b>0.799</b>	<b>0.719</b>	<b>0.724</b>	<b>0.763</b>	<b>0.755</b>	<b>0.763</b>

**Table 4: Comparison of text to motion generation using metrics on artifact.**

Method	sliding (cm/s) ↓	penetration (cm) ↓	floating (cm) ↓
Real	0.743	1.442	0.079
MotionDiffuse[2022]	1.359	1.783	0.051
MDM[2022b]	<b>0.721</b>	1.622	0.102
MLD[2023b]	0.949	2.392	0.064
Ours (LGTM)	0.854	<b>1.247</b>	<b>0.046</b>

**Table 5: Comparison of the impact of different text encoders on full-body metrics computed in the latent space of T2M model [Guo et al. 2022a].**

Method	FID ↓	DIV ↑	R Precision ↑			MM Dist ↓
			Top 1	Top 2	Top 3	
MDM + CLIP	0.747	9.462	0.390	0.581	0.695	3.635
MDM + TMR	<b>0.403</b>	<b>9.687</b>	<b>0.455</b>	<b>0.653</b>	<b>0.759</b>	<b>3.266</b>
Ours + CLIP	0.331	9.386	0.391	0.569	0.674	3.699
Ours + TMR	<b>0.218</b>	<b>9.638</b>	<b>0.490</b>	<b>0.689</b>	<b>0.788</b>	<b>3.013</b>

Table 5 and Table 6 evaluate full-body and part-level motion quality, respectively. In general, we observe that using the TMR text encoder consistently produces better results than using CLIP, for both our method and MDM as well as both local and global quality. When comparing our method to MDM using the same text encoder, our method generally performs better, further demonstrating the superiority of our local-to-global design.

**Table 6: Comparison of the impact of different text encoders on PMM Sim computed using the part-level TRM encoder. The greater the value, the better.**

Method	head	left arm	right arm	torso	left leg	right leg
MDM + CLIP	0.783	0.699	0.691	0.740	0.717	0.723
MDM + TMR	<b>0.803</b>	<b>0.704</b>	<b>0.707</b>	<b>0.756</b>	<b>0.734</b>	<b>0.743</b>
Ours + CLIP	0.795	0.693	0.694	0.752	0.725	0.732
Ours + TMR	<b>0.799</b>	<b>0.719</b>	<b>0.724</b>	<b>0.763</b>	<b>0.755</b>	<b>0.763</b>

**Table 7: Comparison of the impact of using Conformer versus Transformer in Part Motion Encoders on global quality.**

Method	FID ↓	DIV ↑	R Precision ↑			MM Dist ↓
			Top 1	Top 2	Top 3	
Transformer	1.814	8.578	0.373	0.567	0.680	3.688
Conformer	<b>0.218</b>	<b>9.638</b>	<b>0.490</b>	<b>0.689</b>	<b>0.788</b>	<b>3.013</b>

**Table 8: Comparison of the impact of using Conformer versus Transformer in Part Motion Encoders on PMM Sim. Higher values indicate better performance.**

Method	head	left arm	right arm	torso	left leg	right leg
Transformer	0.784	0.712	0.718	0.750	0.728	0.732
Conformer	<b>0.799</b>	<b>0.719</b>	<b>0.724</b>	<b>0.763</b>	<b>0.755</b>	<b>0.763</b>

*The impact of Conformer.* The goal of replacing Transformer with Conformer in Part Motion Encoders is to improve the motion quality. To validate the improvement, we compare both configurations on global quality metrics. From Table 7 and Table 8, we observe that LGTM with Conformer can achieve better quality and semantic matching performance than with Transformer. This improvement can be attributed to the convolution blocks of Conformer, which capture local features better than self-attention.

*The importance of full-body motion optimizer.* The goal of our full-body motion optimizer is to establish correlations among different body part movements and improve the coordination of full-body movements. To validate the effect, we compare it to the setting “w/o opt”, where we remove the key component of our full-body optimizer, namely, the attention encoder. From Table 9 and Table 10, we can see that the local motion quality drops, and the full-body motion quality is also much worse without the optimizer; see Figure 6 for one example result. Without the full-body optimizer, the character’s two feet cannot coordinate well to step alternately during movement due to the lack of information exchange.

## 5 CONCLUSION

In this study, we propose LGTM for text-to-motion generation, which significantly improves the accuracy and coherence of 3D human motion derived from textual descriptions. By integrating large language models with a local-to-global generation framework, our method effectively addresses key challenges in semantic mapping and motion coherence.

**Table 9: Comparison of the impact of attention encoder on global quality. These metric are calculated using the T2M model [Guo et al. 2022a].**

Method	FID ↓	DIV ↑	R Precision ↑			MM Dist ↓
			Top 1	Top 2	Top 3	
w/o opt	7.384	11.552	0.219	0.360	0.454	5.227
w/ opt	<b>0.218</b>	<b>9.638</b>	<b>0.490</b>	<b>0.689</b>	<b>0.788</b>	<b>3.013</b>

**Table 10: Comparison of the impact of attention encoder on PMM Sim using the part-level TMR encoder. The greater the value, the better.**

Method	head	left arm	right arm	torso	left leg	right leg
w/o opt	0.783	0.715	0.700	0.735	0.699	0.709
w/ opt	<b>0.799</b>	<b>0.719</b>	<b>0.724</b>	<b>0.763</b>	<b>0.755</b>	<b>0.763</b>



(a) With full-body optimizer. (b) Without full-body optimizer.

**Figure 6: Motions generation by our method with and without the full-body optimizer for “a person walks upstairs, turns left, and walks back downstairs.”**



**Figure 7: A failure case. The corresponding input prompt is someone imitating a golf swing.**

*Limitation and future work.* As we use ChatGPT for motion description decomposition, the local semantic mapping depends on the reasoning ability of ChatGPT. Incorrect decomposition or mapping may lead to unsatisfactory motion generation results. For example, when generating the “golf swing” motion, which requires high-level and full-body coordination, LGTM struggles because ChatGPT identifies that the right hand swings the golf club but fails to decompose this reasoning into a series of low-level actions for each body part. The result is that the network generates an implausible motion, as shown in Figure 7. Also, ambiguous texts in

the dataset can confuse the network during training. For example, the phrase “a person performs action A and action B” could imply that these actions occur simultaneously or sequentially, leading to output that may not align with user expectations. This issue could be mitigated by providing more detailed temporal descriptions. Furthermore, due to the limited length of samples in the dataset, our current framework cannot consistently generate long-term motions with high quality. For future work, one promising direction is to incorporate our local-to-global idea with those VQ-VAE based approaches such as TM2T [Guo et al. 2022b] and MotionGPT [Jiang et al. 2023] by onstructing part-level motion clips as motion tokens for more detailed motion generation with different part-level motion combinations.

## ACKNOWLEDGMENTS

We thank the anonymous reviewers for their valuable comments. This work was supported in parts by NSFC (62322207, 62161146005, U2001206), Guangdong Natural Science Foundation (2021B1515020085), Shenzhen Science and Technology Program (RCYX20210609103121030), DEGP Innovation Team (2022KCXTD025), Guangdong Laboratory of Artificial Intelligence and Digital Economy (SZ) and Scientific Development Funds of Shenzhen University.

## REFERENCES

- Chaitanya Ahuja and Louis-Philippe Morency. 2019. Language2pose: Natural Language Grounded Pose Forecasting. In *2019 International Conference on 3D Vision (3DV)*. IEEE, 719–728.
- Simon Alexanderson, Rajmund Nagy, Jonas Beskow, and Gustav Eje Henter. 2023. Listen, Denoise, Action! Audio-Driven Motion Synthesis with Diffusion Models. *ACM Transactions on Graphics* 42, 4 (Aug. 2023), 1–20. <https://doi.org/10.1145/3592458>
- Nikos Athanasiou, Mathis Petrovich, Michael J. Black, and Gül Varol. 2022. TEACH: Temporal Action Composition for 3D Humans. In *2022 International Conference on 3D Vision (3DV)*. IEEE Computer Society, 414–423. <https://doi.org/10.1109/3DV57658.2022.00053>
- Jinseok Bae, Jungdam Won, Donggeun Lim, Cheol-Hui Min, and Young Min Kim. 2023. PMP: Learning to Physically Interact with Environments Using Part-wise Motion Priors. In *ACM SIGGRAPH 2023 Conference Proceedings (SIGGRAPH '23)*. Association for Computing Machinery, New York, NY, USA, 1–10. <https://doi.org/10.1145/3588432.3591487>
- Lu Chen, Sida Peng, and Xiaowei Zhou. 2021. Towards Efficient and Photorealistic 3D Human Reconstruction: A Brief Survey. *Visual Informatics* 5, 4 (Dec. 2021), 11–19. <https://doi.org/10.1016/j.visinf.2021.10.003>
- Xin Chen, Biao Jiang, Wen Liu, Zilong Huang, Bin Fu, Tao Chen, and Gang Yu. 2023a. Executing Your Commands via Motion Diffusion in Latent Space. In *2023 IEEE/CVF Conference on Computer Vision and Pattern Recognition (CVPR)*. IEEE, Vancouver, BC, Canada, 18000–18010. <https://doi.org/10.1109/CVPR52729.2023.01726>
- Xin Chen, Biao Jiang, Wen Liu, Zilong Huang, Bin Fu, Tao Chen, Jingyi Yu, and Gang Yu. 2023b. Executing Your Commands via Motion Diffusion in Latent Space. <https://doi.org/10.48550/arXiv.2212.04048> arXiv:2212.04048 [cs]
- Anindita Ghosh, Noshaba Cheema, Cennet Oguz, Christian Theobalt, and Philipp Slusallek. 2021. Synthesis of Compositional Animations From Textual Descriptions. In *Proceedings of the IEEE/CVF International Conference on Computer Vision*. 1396–1406.
- Anmol Gulati, James Qin, Chung-Cheng Chiu, Niki Parmar, Yu Zhang, Jiahui Yu, Wei Han, Shibo Wang, Zhengdong Zhang, Yonghui Wu, and Ruoming Pang. 2020. Conformer: Convolution-augmented Transformer for Speech Recognition. arXiv:2005.08100 [cs, eess]
- Chuan Guo, Shihao Zou, Xinxin Zuo, Sen Wang, Wei Ji, Xingyu Li, and Li Cheng. 2022a. Generating Diverse and Natural 3D Human Motions From Text. In *Proceedings of the IEEE/CVF Conference on Computer Vision and Pattern Recognition*. 5152–5161.
- Chuan Guo, Xinxin Zuo, Sen Wang, and Li Cheng. 2022b. TM2T: Stochastic and Tokenized Modeling for the Reciprocal Generation of 3D Human Motions and Texts. In *Computer Vision – ECCV 2022: 17th European Conference, Tel Aviv, Israel, October 23–27, 2022, Proceedings, Part XXXV*. Springer-Verlag, Berlin, Heidelberg, 580–597. [https://doi.org/10.1007/978-3-031-19833-5\\_34](https://doi.org/10.1007/978-3-031-19833-5_34)

- Chris Hecker, Bernd Raabe, Ryan W. Enslow, John DeWeese, Jordan Maynard, and Kees van Prooijen. 2008. Real-Time Motion Retargeting to Highly Varied User-Created Morphologies. *ACM Transactions on Graphics* 27, 3 (Aug. 2008), 1–11. <https://doi.org/10.1145/1360612.1360626>
- Deok-Kyeong Jang, Soomin Park, and Sung-Hee Lee. 2022. Motion Puzzle: Arbitrary Motion Style Transfer by Body Part. *ACM Transactions on Graphics* (Jan. 2022). <https://doi.org/10.1145/3516429>
- Won-Seob Jang, Won-Kyu Lee, In-Kwon Lee, and Jehhee Lee. 2008. Enriching a Motion Database by Analogous Combination of Partial Human Motions. *The Visual Computer* 24, 4 (April 2008), 271–280. <https://doi.org/10.1007/s00371-007-0200-1>
- Biao Jiang, Xin Chen, Wen Liu, Jingyi Yu, Gang Yu, and Tao Chen. 2023. MotionGPT: Human Motion as a Foreign Language. <https://doi.org/10.48550/arXiv.2306.14795> arXiv:2306.14795 [cs]
- Chong Lan, Yongsheng Wang, Chengze Wang, Shirong Song, and Zheng Gong. 2023. Application of ChatGPT-Based Digital Human in Animation Creation. *Future Internet* 15, 9 (Sept. 2023), 300. <https://doi.org/10.3390/fi15090300>
- Seyoung Lee, Jiye Lee, and Jehhee Lee. 2022. Learning Virtual Chimeras by Dynamic Motion Reassembly. *ACM Transactions on Graphics* 41, 6 (Nov. 2022), 182:1–182:13. <https://doi.org/10.1145/3550454.3555489>
- Matthew Loper, Naureen Mahmood, Javier Romero, Gerard Pons-Moll, and Michael J. Black. 2015. SMPL: A Skinned Multi-Person Linear Model. *ACM Transactions on Graphics* 34, 6 (Oct. 2015), 248:1–248:16. <https://doi.org/10.1145/2816795.2818013>
- Mathis Petrovich, Michael J. Black, and Gül Varol. 2022. TEMOS: Generating Diverse Human Motions from Textual Descriptions. In *Computer Vision – ECCV 2022: 17th European Conference, Tel Aviv, Israel, October 23–27, 2022, Proceedings, Part XXII*. Springer-Verlag, Berlin, Heidelberg, 480–497. [https://doi.org/10.1007/978-3-031-20047-2\\_28](https://doi.org/10.1007/978-3-031-20047-2_28)
- Mathis Petrovich, Michael J. Black, and Gül Varol. 2023. TMR: Text-to-Motion Retrieval Using Contrastive 3D Human Motion Synthesis. arXiv:2305.00976 [cs]
- Ben Poole, Ajay Jain, Jonathan T. Barron, and Ben Mildenhall. 2022. DreamFusion: Text-to-3D Using 2D Diffusion. <https://doi.org/10.48550/arXiv.2209.14988> arXiv:2209.14988 [cs, stat]
- Alec Radford, Jong Wook Kim, Chris Hallacy, Aditya Ramesh, Gabriel Goh, Sandhini Agarwal, Girish Sastry, Amanda Askell, Pamela Mishkin, Jack Clark, Gretchen Krueger, and Ilya Sutskever. 2021. Learning Transferable Visual Models From Natural Language Supervision. <https://doi.org/10.48550/arXiv.2103.00020> arXiv:2103.00020 [cs]
- Robin Rombach, Andreas Blattmann, Dominik Lorenz, Patrick Esser, and Bjorn Ommer. 2022. High-Resolution Image Synthesis with Latent Diffusion Models. In *2022 IEEE/CVF Conference on Computer Vision and Pattern Recognition (CVPR)*. IEEE, New Orleans, LA, USA, 10674–10685. <https://doi.org/10.1109/CVPR52688.2022.01042>
- Mark Scanlon, Frank Breiting, Christopher Hargreaves, Jan-Niclas Hilgert, and John Sheppard. 2023. ChatGPT for Digital Forensic Investigation: The Good, the Bad, and the Unknown. *Forensic Science International: Digital Investigation* 46 (Oct. 2023), 301609. <https://doi.org/10.1016/j.fsidi.2023.301609>
- Asako Soga, Yuho Yazaki, Bin Umino, and Motoko Hirayama. 2016. Body-Part Motion Synthesis System for Contemporary Dance Creation. In *ACM SIGGRAPH 2016 Posters*. ACM, Anaheim California, 1–2. <https://doi.org/10.1145/2945078.2945107>
- Jiaming Song, Chenlin Meng, and Stefano Ermon. 2022. Denoising Diffusion Implicit Models. <https://doi.org/10.48550/arXiv.2010.02502> arXiv:2010.02502 [cs]
- Sebastian Starke, He Zhang, Taku Komura, and Jun Saito. 2019. Neural State Machine for Character-Scene Interactions. *ACM Transactions on Graphics* 38, 6 (Nov. 2019), 209:1–209:14. <https://doi.org/10.1145/3355089.3356505>
- Sebastian Starke, Yiwei Zhao, Taku Komura, and Kazi Zaman. 2020. Local Motion Phases for Learning Multi-Contact Character Movements. *ACM Transactions on Graphics* 39, 4 (July 2020), 54:1–54:13. <https://doi.org/10.1145/3386569.3392450>
- Sebastian Starke, Yiwei Zhao, Fabio Zinno, and Taku Komura. 2021. Neural Animation Layering for Synthesizing Martial Arts Movements. *ACM Transactions on Graphics* 40, 4 (July 2021), 92:1–92:16. <https://doi.org/10.1145/3450626.3459881>
- Guy Tevet, Brian Gordon, Amir Hertz, Amit H. Bermano, and Daniel Cohen-Or. 2022a. MotionCLIP: Exposing Human Motion Generation to CLIP Space. In *Computer Vision – ECCV 2022 (Lecture Notes in Computer Science)*, Shai Avidan, Gabriel Brostow, Moustapha Cissé, Giovanni Maria Farinella, and Tal Hassner (Eds.). Springer Nature Switzerland, Cham, 358–374. [https://doi.org/10.1007/978-3-031-20047-2\\_21](https://doi.org/10.1007/978-3-031-20047-2_21)
- Guy Tevet, Sigal Raab, Brian Gordon, Yoni Shafir, Daniel Cohen-or, and Amit Haim Bermano. 2022b. Human Motion Diffusion Model. In *The Eleventh International Conference on Learning Representations*.
- Ashish Vaswani, Noam Shazeer, Niki Parmar, Jakob Uszkoreit, Llion Jones, Aidan N Gomez, Łukasz Kaiser, and Illia Polosukhin. 2017. Attention Is All You Need. In *Advances in Neural Information Processing Systems*, Vol. 30. Curran Associates, Inc.
- Heyuan Yao, Zhenhua Song, Yuyang Zhou, Tenglong Ao, Baoquan Chen, and Libin Liu. [n. d.]. MoConVQ: Unified Physics-Based Motion Control via Scalable Discrete Representations. ([n. d.]).
- Ye Yuan, Jiaming Song, Umar Iqbal, Arash Vahdat, and Jan Kautz. 2022. PhysDiff: Physics-Guided Human Motion Diffusion Model. <https://doi.org/10.48550/arXiv.2212.02500> arXiv:2212.02500 [cs]
- Ailing Zeng, Lei Yang, Xuan Ju, Jiefeng Li, Jianyi Wang, and Qiang Xu. 2022. SmoothNet: A Plug-and-Play Network for Refining Human Poses in Videos. In *European Conference on Computer Vision*. Springer.
- He Zhang, Sebastian Starke, Taku Komura, and Jun Saito. 2018. Mode-Adaptive Neural Networks for Quadruped Motion Control. *ACM Transactions on Graphics* 37, 4 (July 2018), 145:1–145:11. <https://doi.org/10.1145/3197517.3201366>
- Mingyuan Zhang, Zhongang Cai, Liang Pan, Fangzhou Hong, Xinying Guo, Lei Yang, and Ziwei Liu. 2022. MotionDiffuse: Text-Driven Human Motion Generation with Diffusion Model. arXiv:2208.15001 [cs]
- Yuheng Zhao, Jinjing Jiang, Yi Chen, Richen Liu, Yalong Yang, Xiangyang Xue, and Siming Chen. 2022. Metaverse: Perspectives from Graphics, Interactions and Visualization. *Visual Informatics* 6, 1 (March 2022), 56–67. <https://doi.org/10.1016/j.visinf.2022.03.002>